J. Physiol. (1987), **387**, *pp.* 251–272
With 11 *text-figures*
Printed in Great Britain

VOLTAGE-DEPENDENT MAGNESIUM BLOCK OF ADENOSINE-TRIPHOSPHATE-SENSITIVE POTASSIUM CHANNEL IN GUINEA-PIG VENTRICULAR CELLS

BY MINORU HORIE, HIROSHI IRISAWA AND AKINORI NOMA*

From the National Institute for Physiological Sciences, Myodaiji, Okazaki 444, Japan

SUMMARY

1. The adenosine-5′-triphosphate (ATP)-sensitive K^+ channel of guinea-pig ventricular cells was examined in the presence and absence of internal Mg^{2+} or Na^+ using an open cell-attached configuration of the patch-clamp technique.

2. Millimolar concentrations of internal Mg^{2+} ($[Mg^{2+}]_i$) produced marked fluctuations in the outward current, and the amplitude of the open-channel current was reduced with increasing $[Mg^{2+}]_i$. Millimolar Na^+ applied internally also decreased the mean amplitude of the outward current, but the increase in current noise was not obvious. These effects became larger when the membrane potential was shifted to be more positive from the K^+ equilibrium potential (E_K). At potentials negative to E_K the inward current was affected by neither internal Mg^{2+} nor Na^+.

3. The external application of Na^+, Mg^{2+} or Ca^{2+}, however, failed to affect the single-channel current.

4. After removal of both internal Mg^{2+} and Na^+, the mean open-channel current–voltage relationship became virtually linear. Referring to these unblocked values, relative amplitudes were determined at different levels of $[Mg^{2+}]_i$ or $[Na^+]_i$. The dose–response relations gave a Hill coefficient of ~ 1 for Mg^{2+} block and ~ 2 for Na^+ block. The half-maximum concentrations (K_h) for both Mg^{2+} and Na^+ block were shifted to lower values with increasing positive potentials.

5. The power-density spectrum of the open-channel current noise induced by internal Mg^{2+} showed a Lorentzian function with a corner frequency above 1 kHz, suggesting that the current noise is due to rapid fluctuations of open-channel current between blocked and unblocked states. The corner frequencies gave Mg^{2+} block and unblock rate constants which were of the order of 10^7 M^{-1} s^{-1} and 10^4 s^{-1}, respectively.

6. With increasing external K^+ concentration ($[K^+]_o$) from 0 to 140 mM the current fluctuations became less prominent, and K_h for Mg^{2+} block was shifted to higher values. Raising $[K^+]_o$ enhanced the unblock rate derived from the noise analysis while the block rate was not significantly altered.

7. The above findings could be explained by assuming a binding site for one Mg^{2+} or two Na^+ located 30–35 % of the electrical drop across the membrane from the inner mouth of the channel, thereby resulting in the ionic block of K^+ passage. An apparent inward rectification observed in the single-channel current–voltage relation is attributable to the blockade of the channel by intracellular Mg^{2+} and/or Na^+.

* Present address: Department of Physiology, Faculty of Medicine, Kyushu University, Fukuoka 812, Japan.

INTRODUCTION

In mammalian heart cells an inwardly rectifying K^+-selective channel that opens at low intracellular concentrations of adenosine 5′-triphosphate (ATP) has been investigated by using the patch-clamp technique (Noma, 1983; Kakei & Noma, 1984; Trube & Hescheler, 1984; Kakei, Noma & Shibasaki, 1985; Noma & Shibasaki, 1985). One of the well-known properties of this channel is a decrease of the 'unitary amplitude' (negative slope) on strong depolarization from the K^+ equilibrium potential (E_K; see Fig. 2 of Noma, 1983) when measured in both cell-attached and cell-free configurations. This property has also been found in the ATP-sensitive K^+ channels of pancreatic β cells and skeletal muscle fibres (Cook & Hales, 1984; Ashcroft, Harrison & Ashcroft, 1984; Spruce, Standen & Stanfield, 1985; Rorsman & Trube, 1985). Thus, as the membrane potential is made more positive to E_K, the current–voltage curve for the outward current gradually deviates from the linear relationship which is extrapolated from the inward-going current.

As a mechanism for the negative slope, it has been reported that internal blockers such as Na^+ and tetraethylammonium (TEA^+) can plug the channel and induce an inward rectification of the channel (Cook & Hales, 1984; Kakei *et al.* 1985). Similar Na^+ block has been observed in K^+ channels of other classes, where the current–voltage relations became linear when Na^+ were eliminated from the inside of the membrane (Bergman, 1970; Bezanilla & Armstrong, 1972; French & Wells, 1977; Marty, 1983; Yellen, 1984*a*, *b*). In the ATP-sensitive K^+ channel, however, the rectification remained after the complete removal of internal Na^+ in the inside-out patches (Kakei *et al.* 1985), and thus a blocking effect of other cations such as Mg^{2+} in the internal solutions was suspected.

In the present study we observed that the ATP-sensitive K^+ channel showed linear current–voltage relations after the removal of both Mg^{2+} and Na^+ from the inside of the membrane. Our results indicate that physiological concentrations of internal Mg^{2+} can block the outward current through the ATP-sensitive K^+ channel, thereby resulting in a negative slope of the conductance at positive potentials.

Some of these results have appeared previously in abstract form (Horie, Noma & Irisawa, 1986).

METHODS

Preparations. Single ventricular cells were dissociated by treating adult guinea-pig hearts with collagenase, followed by incubation in enzyme-free high-K^+, low-Ca^{2+} medium (Isenberg & Klöckner, 1982). The procedure of collagenase treatment was essentially the same as in previous reports (Powell, Terrar & Twist, 1980; Taniguchi, Kokubun, Noma & Irisawa, 1981).

Solutions. The compositions of Tyrode, pipette, and internal solutions are listed in Table 1. To exclude the blocking kinetics of ATP from kinetic analysis of the channel current, and also to prolong the open time of the ATP-sensitive K^+ channel, ATP was omitted from the internal solution in most experiments. When the background noise in the absence of the channel activity was recorded, an internal solution containing 2–3 mM-ATP was perfused in the chamber. To prepare internal solutions containing 0·1–10 mM-free Mg^{2+}, an appropriate amount of $MgCl_2$ was added to the standard internal solution according to Fabiato & Fabiato (1979) using the correction of Tsien & Rink (1980). The Na^+ test solutions were prepared by adding NaCl to the standard internal solution. When the effects of external divalent cations on the channel were examined, 2 mM-$CaCl_2$

in the pipette was replaced with 5 mM-$MgCl_2$ or 5 mM-EGTA, without correcting the osmolarity. The pH was adjusted to 7·4 with HEPES–KOH buffer before the experiment.

Open cell-attached inside-out patch-clamp technique. To keep intact the connection of the patch membrane to the intracellular structure during inside-out patch recording (Hamill, Marty, Neher, Sakmann & Sigworth, 1981), the modified open cell-attached patch method was used (Kakei *et al.* 1985; Noma & Shibasaki, 1985). Briefly, the 'gigohm' seal was established near the centre of the cell in the control Tyrode solution, then Ca^{2+} was washed out from the chamber by perfusing Ca^{2+}-free Tyrode solution (Table 1) for 2–3 min, which was followed by a perfusion of an internal solution. This procedure prevented the contraction of the cell on depolarization when the Na^+-rich bath solution was switched to a K^+-rich one. The cell membrane was ruptured by crushing a part of the cell between the bottom of the recording chamber and a glass-pipette tip, which had the

TABLE 1. Composition of solutions (mM)

Tyrode solutions

	NaCl	NaH_2PO_4	KCl	$CaCl_2$	$MgCl_2$	HEPES
Normal	136·5	0·3	5·4	1·8	0·5	5
Ca^{2+}-free	136·5	0·3	5·4	—	0·5	5

Pipette solutions

	KCl	$CaCl_2$	$MgCl_2$	EGTA	HEPES
Standard	140	2	—	—	5
5 mM-Mg^{2+}	140	—	5	—	5
5 mM-EGTA	140	—	—	5	5

Internal solutions

	KCl	NaCl	$MgCl_2$	EGTA	HEPES
Standard	140	—	—	1	5
Mg^{2+} test	140	—	0·1–10	—	5
Na^+ test	140	5–50	—	—	5

EGTA: ethyleneglycol-bis(β-aminoethylether)*N*,*N*′-tetracetic acid (Dotide), HEPES: *N*-2-hydroxyethylpiperazine-*N*′-2-ethanesulphonic acid (Dotide). The pH of all solutions was adjusted to 7·4 with KOH. Mg^{2+} test solutions were prepared by adding the appropriate amount of $MgCl_2$ to the standard solution according to Fabiato & Fabiato (1979) with a correction by Tsien & Rink (1980).

same shape as that used for the patch electrode. When the cells attached firmly to the bottom of the chamber, the procedure of crushing the cell did not dislodge the patch electrode, although the tip of the glass pipette used for crushing was broken. The cell milieu was equilibrated with the bathing solution through the hole made on the surface membrane. The pipette used for crushing the cell was withdrawn out of the chamber during the experiment. After disruption of the cell membrane, the ATP-sensitive K^+ channel appeared within 30 s, when the ATP concentration in the internal solution was below 2 mM. At room temperature (T = 24 °C) the channel activity was maintained for as long as 30 min even in the ATP-free test solutions. Although patches were occasionally found to be isolated because of contracture of the cell, a few channels remained active. The bath solution was grounded through an agar/Ag–AgCl bridge, and the pipette potential was clamped at various levels. Membrane potentials in this paper indicate transmembrane potentials at the inside of the cell membrane.

Data analysis. The single-channel currents from open cell-attached patches were recorded using a patch-clamp amplifier (EPC7, List, Darmstadt, F.R.G.) and stored on video tape (T120, Victor, Tokyo, Japan) through a pulse code modulation system (RP 880, NF, Tokyo, Japan) for later analysis with a computer (E-600, Hitachi, Japan). The frequency response of the recording system was flat up to 15 kHz, which is above the upper limit of frequency domain in our noise analysis. High-frequency signals of the channel current, however, were slightly damped near 15 kHz by the stray capacitance along the input line including the electrode. To minimize this effect, the shank of the pipette (3–5 MΩ) was coated with silicone.

To evaluate Mg^{2+} or Na^+ as an open-channel blocker, we computed the mean amplitude of the

open-channel current, $\bar{i}$, from digital records. $\bar{i}$ is a product of the probability that the channel is unblocked during the open state (p) and the unit amplitude of the single-channel current (i). The current signal was fed from the video tape to the computer via a Bessel-type low-pass filter (48 dB octave^{-1} with cut-off frequency of 3 kHz, FV-625A, NF) and sampled every 0·3 ms. Then the current records were divided into segments of base-line currents (closed state of the channel) and of open-channel current, and the average was calculated for each group of segments. The value of $\bar{i}$ was measured as the difference of the two averages. Segments of base line continuing for longer than 30 ms were selected for calculation. The open state of the channel was tentatively assumed to be terminated when current level stepped from the open-channel current level to the base line and stayed longer than the critical time of 1 ms. Brief closure of the channel was assumed to be due to blockade of the open-state channel. In preliminary measurements we changed the critical time for discriminating the channel state between 0·3 and 2·1 ms, but the value of $\bar{i}$ was not significantly altered.

Power-density spectrum analysis. For the noise analysis, relatively wide-tipped pipettes (< 2 MΩ) were used. The cut-off frequency of the Butterworth type active filter was set at 12 kHz, through which the data were fed into memory array in the computer with sampling time of 50 μs. The power-density spectrum was calculated by using a fast Fourier transformation (one-sided power spectrum) for each data frame of 1024 points and displayed in log–log coordinates after averaging 20–40 frames. Spectra of background noise were calculated from frames without channel openings and their average was subtracted from the frames containing mainly channel openings. In order to minimize the component due to open and close kinetics of the channel, data frames that showed obvious step-like transition between closed and open states were excluded from the calculation of the average spectrum.

The difference spectrum was fitted to a Lorentzian function, $S(f) = S(0)/(1+(f/f_c)^2)$, where $S(f)$ is the spectral density of the measured current fluctuations at a given frequency (f) and f_c is the corner frequency giving a half of $S(0)$ (Anderson & Stevens, 1973), by calculating a least-squares sum of the difference between the theoretical curve and a part of the spectrum where the blocking kinetics was considered to dominate (Colquhoun, 1971). The Lorentzian component generated by the blocking kinetics of the channel showed a corner frequency higher than 1 kHz and was clearly separated from the component due to intrinsic gating kinetics of the channel, which showed a corner frequency of less than 10 Hz (see Fig. 6, Noma & Shibasaki, 1985). All experiments were carried out at 34–35 °C or at room temperature (about 24 °C). Numerical data are expressed as mean ±S.D.

RESULTS

Unidirectional block of the ATP-sensitive K^+ channel by intracellular Mg^{2+}

Both inward and outward currents through the ATP-sensitive K^+ channel were recorded with 140 mM-K^+ on both sides of the patch membrane in the open cell-attached patch configuration. Fig. 1*A* illustrates single-channel currents at +40 and −40 mV in the absence and presence of internal Mg^{2+} at different concentrations ($[Mg^{2+}]_i$). In its absence the outward current was almost equal to the inward current, indicating ohmic conductance for both directions. As $[Mg^{2+}]_i$ was elevated, the mean amplitude of the open-channel current, $\bar{i}$, in the inward direction remained constant, whereas the outward current became smaller. These relationships were represented by the downward curvature of the relationship between $\bar{i}$ and the membrane potential (E_m) with the higher $[Mg^{2+}]_i$ and the larger clamp steps (Fig. 1*B*). The depression of the outward current was completely reversible on washing out the internal Mg^{2+}.

Similar Mg^{2+} effects were observed in other experiments. The value of $\bar{i}$ with concentrations of 0, 2 and 5 mM internal Mg^{2+} at +40 mV was 2·7±0·3 pA (n = 12), 1·7±0·5 pA (n = 7) and 1·1±0·3 pA (n = 8) respectively; its value with the same concentrations at −40 mV was −3·0±0·3 pA, −3·2±0·8 pA and −2·9±0·4 pA, respectively, indicating that the mean inward currents at −40 mV were not

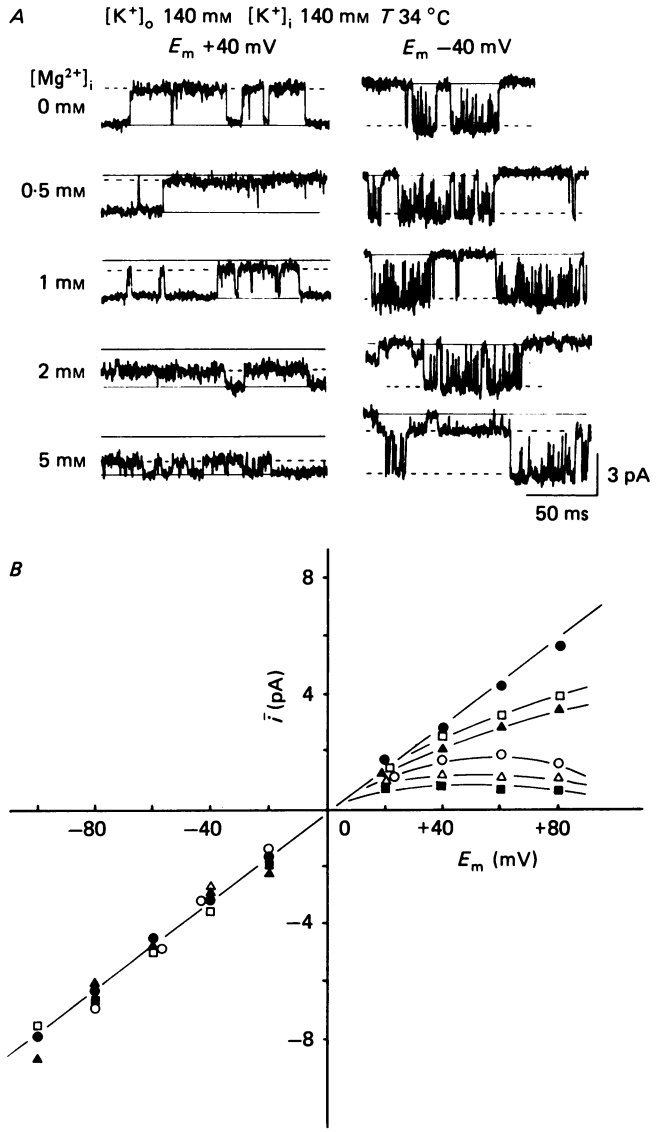

Fig. 1. Effect of internal Mg^{2+} on the ATP-sensitive K^+ channel. *A*, original current traces recorded from the same patch at $[Mg^{2+}]_i$ of 0, 0·5, 1, 2 and 5 mM under symmetrical ionic K^+ solutions (140 mM, 34 °C). The current zero level is indicated by a continuous line and the mean amplitude of open-channel current ($\bar{i}$) by a dotted line. In the left column, the open-channel current level in absence of internal Mg^{2+} is also indicated by continuous lines. In the bottom two traces of the right column, openings of the inward-rectifier K^+ channel are also seen, and overlap with those of the ATP-sensitive K^+ channel. Low-pass filter was 5 kHz. When compared to the mean current measured in absence of internal Mg^{2+}, the mean amplitudes of the outward current (left column) at $[Mg^{2+}]_i$ of 0·5, 1, 2 and 5 mM were 92, 75, 48 and 40 %, respectively, at membrane potential (E_m) +40 mV. By contrast, the mean inward currents (right column) measured at the same levels of $[Mg^{2+}]_i$ were 98, 96, 97 and 100% respectively at −40 mV. *B*, current–voltage relations at each $[Mg^{2+}]_i$ obtained from the current data shown in *A*. Symbols: ●, $[Mg^{2+}]_i$ 0 mM; □, 0·5 mM; ▲, 1 mM; ○, 2 mM; △, 5 mM; ■, 10 mM.

significantly affected. The above findings can be explained as follows: internal Mg^{2+} can enter the inner mouth of the ATP-sensitive K^+ channel, but it cannot pass through the channel and thereby prevents K^+ from crossing the channel.

To examine whether Mg^{2+} can enter the channel from the outer mouth of the channel and block it, 5 mM-Mg^{2+} was added to the pipette solution (Fig. 2*A*). The

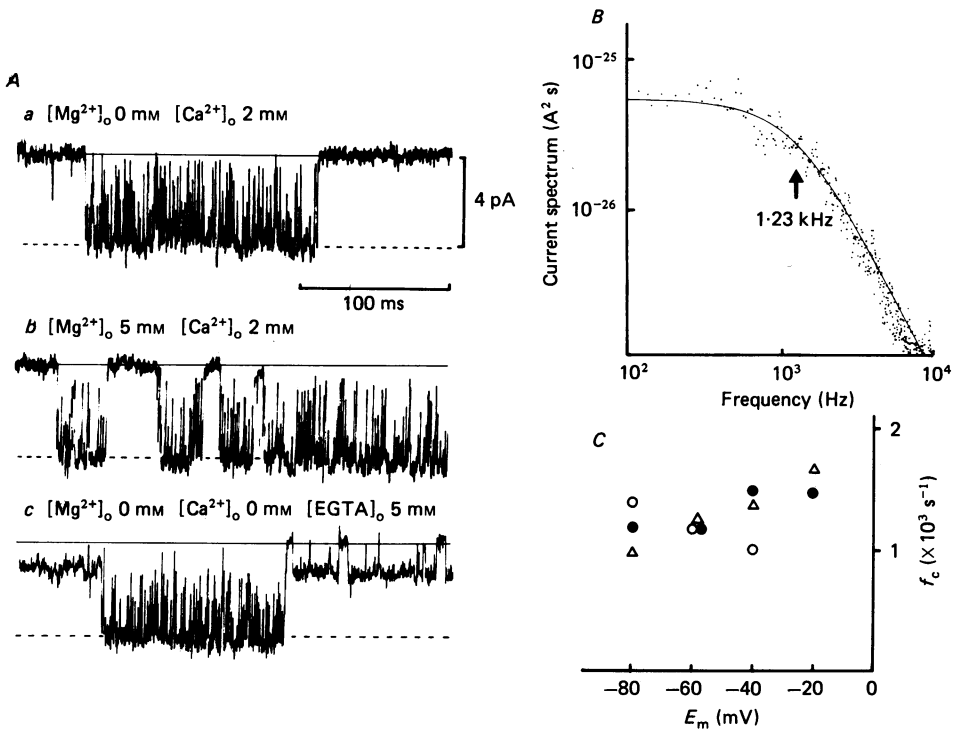

Fig. 2. Effect of external cations on the inward currents. *A*, original traces of the inward currents measured at −60 mV with standard internal solution (140 mM-K^+) and a given pipette (external) solution: *a*, standard (2 mM-Ca^{2+}); *b*, 5 mM-Mg^{2+}; *c*, 5 mM-EGTA (Table 1). Continuous lines indicate the closed state, and dotted lines the mean amplitude of open-channel current. In the bottom trace, the inward-rectifier K^+ channel is also active with relatively smaller amplitude and longer openings. *B*, difference spectrum calculated from inward current fluctuations during the burst gives consistently a Lorentzian function ($S(f) = S(0)/(1+(f/f_c)^2)$) with a corner frequency (f_c) around 1·2 kHz, where $S(f)$ means the current spectrum at a given frequency. *C*, values of f_c obtained from three different patches plotted against the membrane potential (E_m). ○, f_c measured with the standard external solution, i.e. 2 mM-Ca^{2+} (*a*); ●, with 5 mM-Mg^{2+} (*b*); △, with 5 mM-EGTA (*c*). Between −80 and −20 mV, they did not vary significantly irrespective of the presence or the absence of Mg^{2+} or Ca^{2+} in the pipette.

average single-channel conductance was 78·9 ± 4·3 pS ($n = 7$) in the absence of Mg^{2+} and 75·5 ± 6·0 pS ($n = 4$, 34 °C) when the external Mg^{2+} concentration ($[Mg^{2+}]_o$) was 5 mM (Fig. 2*Aa* and *b*); thus external Mg^{2+} does not affect the mean amplitude of the inward current. It is concluded that Mg^{2+} blocks the ATP-sensitive K^+ channel only from the inside of the channel. Thus the effect is unidirectional and voltage dependent.

Fluctuations of the inward-going single-channel current

To determine whether external Ca^{2+} might induce the marked fluctuations observed in the inward-going currents, current fluctuations were compared with or without Ca^{2+} in the external solutions (Fig. 2*Ab* and *c*). The flickery inward current through the ATP-sensitive K^+ channel and the mean amplitudes were quite similar under these conditions.

The inward-going current was also analysed by measuring the power-density spectrum. The power-density spectrum from the burst-like inward current consistently gave a single Lorentzian component with a corner frequency (f_c) of around 1·2 kHz (Fig. 2*B*). The value of f_c did not vary, irrespective of the presence or the absence of external Mg^{2+} or Ca^{2+} (Fig. 2*C*). It is concluded that the flicker of the inward current is not influenced by external Ca^{2+} or Mg^{2+}, and may be attributable to intrinsic gating kinetics of the ATP-sensitive K^+ channel.

Block of the ATP-sensitive K^+ channel by internal Mg^{2+} depends on the net K^+ flux

In order to get more insight into the voltage dependence of the Mg^{2+} block, we varied the reversal potential of the K^+ current. Fig. 3*A* illustrates the single-channel currents at five different internal Mg^{2+} concentrations at 0 mV in the presence of external K^+ at a concentration of 5·4 mM. The open-channel current showed more prominent flicker compared to that recorded at $[K^+]_o$ of 140 mM in Fig. 1*A*. The current–voltage relations at $[Mg^{2+}]_i$ of 0 mM (control) and 2 mM indicate that $\bar{i}$ was reduced as $[Mg^{2+}]_i$ was increased (Fig. 3*B*) and the block of the channel is limited to the membrane potentials positive to E_K.

The value of $\bar{i}$ was normalized by referring to that measured in the absence of internal Mg^{2+} ($\bar{i}/i_0$) at the same membrane potential and was plotted against $[Mg^{2+}]_i$ in Fig. 3*C*. At every membrane potential the relationship was well fitted to saturation kinetics,

$$\bar{i}/i_0 = 1/(1+([Mg^{2+}]_i/K_h)^n), \quad (1)$$

with a Hill coefficient of $n = \sim 1$. The value of $[Mg^{2+}]_i$ which gave the half-saturation (K_h) was dependent on the membrane potential and was shifted to higher concentration as the potential became less positive. At +40 mV and 0 mV, K_h was about 0·5 and 2·0 mM, respectively.

We further examined the relation between $[K^+]_o$ and Mg^{2+} block using pipette solutions containing three different levels of $[K^+]_o$ (0; 20 mM, $E_K = -49$ mV; and 140 mM, $E_K = 0$ mV; 25 °C). In Fig. 4*A*, three original current traces recorded in the presence of internal Mg^{2+} at 0·5 mM at +40 mV are illustrated with respective amplitude histograms. Lowering $[K^+]_o$ from 140 to 0 mM increased the open-channel current fluctuations and gave a broader amplitude distribution, indicating that the block of the channel is accelerated by decreasing $[K^+]_o$. Fig. 4*B* shows dose–response curves measured at +40 mV with four different levels of $[K^+]_o$ (0, 5·4, 20 and 140 mM). They were shifted to the right when $[K^+]_o$ was increased, whereby K_h was increased from about 0·4 mM in absence of K^+ to 2·0 mM when $[K^+]_o$ was 140 mM. All curves were fitted by the eqn. (1) having a slope of $n = 1$. These findings indicate that the influx of K^+ through the channel can knock out Mg^{2+} from its binding site and relieve

the blockade of the K^+ channel; they are consistent with previous observations for tetraethylammonium (TEA^+) and Na^+ block in other K^+ channels (Armstrong, 1971; Bezanilla & Armstrong, 1972; French & Wells, 1977; Marty, 1983; Yellen, 1984*b*).

In Fig. 4*C* the single-channel conductance (γ) at 24 °C is plotted at various levels of $[K^+]_o$ on a log–log scale. When γ was estimated under conditions free from internal blockers, where the current–voltage relation showed a good linearity, raising $[K^+]_o$ increased γ in a dose-dependent manner.

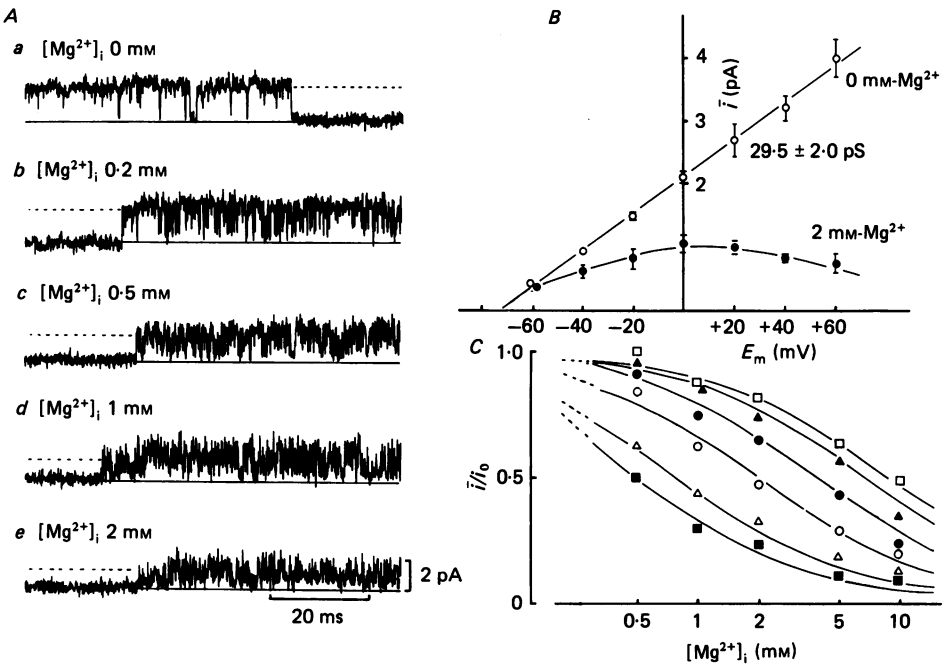

Fig. 3. Mg^{2+} block at $[K^+]_o$ 5·4 mM. *A*, original traces of outward current (low-pass filter of 10 kHz, $E_m = 0$ mV) at $[Mg^{2+}]_i$ 0, 0·2, 0·5, 1 and 2 mM, under $[K^+]_o$ 5·4 mM and $[K^+]_i$ 140 mM (24 °C). The closed-current level is indicated by continuous lines and the mean amplitudes of open-channel current ($\bar{i}$) by dotted lines. In the presence of internal Mg^{2+} rapid fluctuations during the channel openings are visible. *B*, current–voltage relationships at $[Mg^{2+}]_i$ 0 and 2 mM. Vertical bars indicate the standard deviation of $\bar{i}$ ($n = 5$). In absence of internal Mg^{2+} the relationship became linear and the single-channel conductance was 29·5 ± 2·0 pS ($n = 5$). $[Mg^{2+}]_i$ for half-maximum effects (K_h) at +40 mV was about 0·5 mM, which was approximately one-quarter of that estimated at $[K^+]_o$ 140 mM (Fig. 1*B*). *C*, relationships between $\bar{i}/i_0$ and $[Mg^{2+}]_i$ obtained from the same patch at different values of membrane potential gave a Hill coefficient of 1 at $[K^+]_o$ 5·4 mM. Smooth curves are derived from eqn. (1). Symbols: ■, +40 mV; △, +20 mV; ○, 0 mV; ●, −20 mV; ▲, −40 mV; □, −60 mV.

Effects of lowering the temperature on channel kinetics

The kinetics of the flickery channel blockade was measured at low temperature, which may be expected to slow down the kinetics and facilitate the analysis. Therefore, the effect on the K^+ channel of lowering temperature from 34 to 24 °C was first examined. The single-channel conductance of the ATP-sensitive K^+ channel ($[K^+]_o$ 5·4 mM) in the absence of Mg^{2+} and Na^+ was decreased from 38·5 ± 2·8 ($n = 7$)

to 29·5 ± 2·0 pS (n = 5). The temperature coefficient (Q_{10}) was 1·3, corresponding to an activation energy of 5 kcal mol^{-1}, which was of the same order as reported in the anomalous rectifier K^+ channel of starfish egg cell (Q_{10} = 1·62: Hagawara & Yoshii, 1980) and of tunicate egg cell (1·5: Fukushima, 1982).

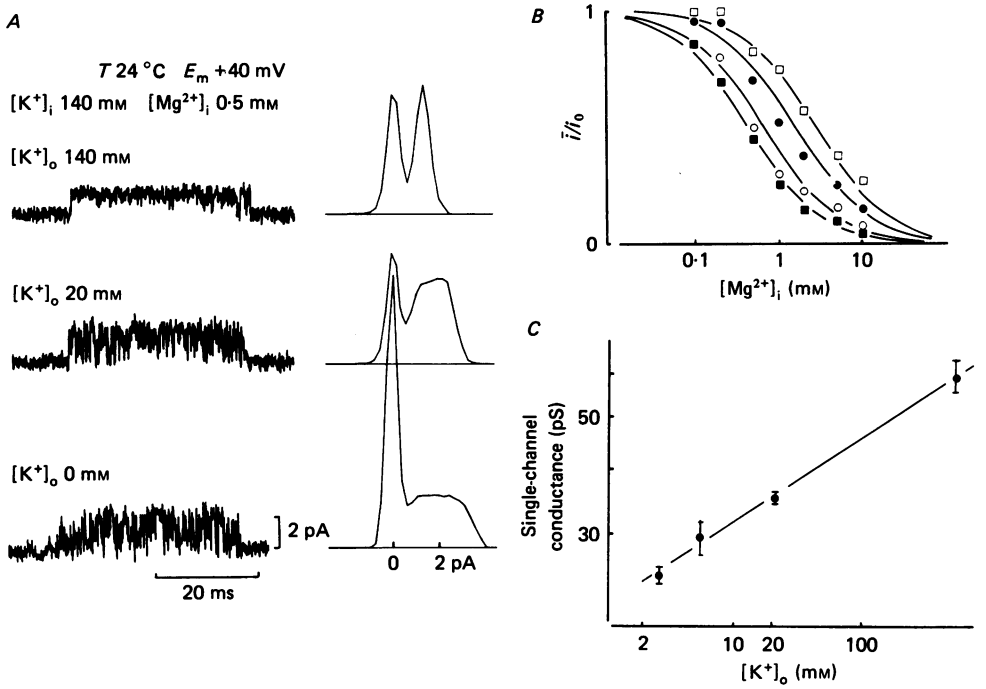

Fig. 4. Mg^{2+} block depends on $[K^+]_o$. *A*, current traces at +40 mV in the presence of 0·5 mM-internal Mg^{2+} were sampled at 10 kHz. Through a Bessel-type active filter with a cut-off frequency of 2 kHz, amplitude histograms were calculated from each current record as shown to the right. *B*, dose–response curves measured at +40 mV at various levels of $[K^+]_o$ (0, 5·4, 20 and 140 mM, four patches) clearly show that raising $[K^+]_o$ shifted K_h to higher values, suggesting relief of Mg^{2+} block. The value of K_h was about 0·4 mM at $[K^+]_o$ 0 mM (■), 0·5 mM at $[K^+]_o$ 5·4 mM (○), 0·8 mM at $[K^+]_o$ 20 mM (●) and 2·0 mM at $[K^+]_o$ 140 mM (□), respectively. All curves are fitted by eqn. (1) having a slope of n = 1. *C*, single-channel conductance (γ) measured in absence of internal Mg^{2+} and internal Na^+ are plotted against $[K^+]_o$. The line was drawn by the equation: $\gamma = 20\ ([K^+]_o)^{0.22}$ pS. The vertical bars of each conductance plot indicate the standard deviation (n = 2 at $[K^+]_o$ 2·7 mM, n = 14 at $[K^+]_o$ 5·4 mM, n = 8 at $[K^+]_o$ 20 mM and n = 21 at $[K^+]_o$ 140 mM, respectively).

With decrease of the temperature of the bathing solution containing 140 mM-K^+ and 0·5 mM-Mg^{2+} from 34 to 24 °C, the mean burst time determined by open-time histograms was prolonged considerably from 142 ± 15 to 203 ± 12 ms ($[K^+]_o$ 5·4 mM at 0 mV, Q_{10} 1·43), but the flicker of the open-channel current during the bursts remained apparently unchanged and it was impossible to analyse the blocking kinetics by measuring the open- and closed-time histograms. Therefore, we decided to examine the kinetics by using noise analysis.

Power-density spectrum of the outward-going single-channel current fluctuations induced by internal Mg^{2+}

The long openings of the channel at 24 °C made it easier to select frames of records which contained only open-channel currents as shown in the inset of *a* in Fig. 5. The average power-density spectrum calculated from such open-channel currents in the presence of 0·2 mM-internal Mg^{2+}, showed a shoulder near 1 kHz. The spectral density

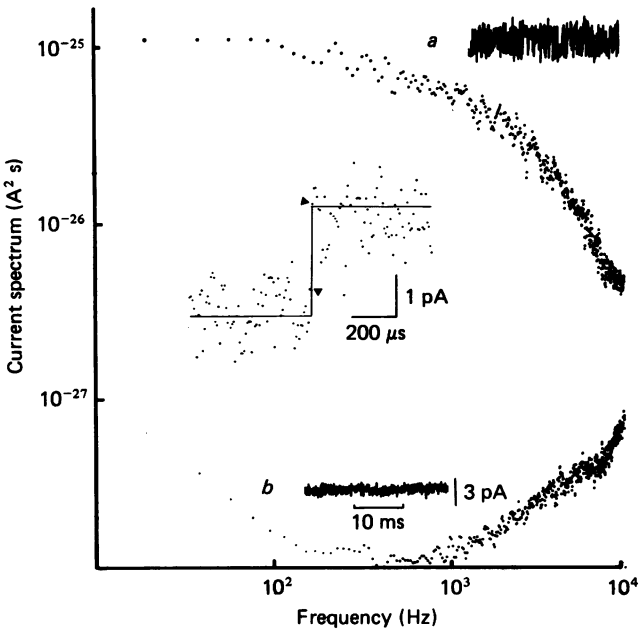

Fig. 5. Noise analysis of outward current fluctuations. Two average power-density spectra measured at +20 mV ($[K^+]_o$ 5·4 mM, 24 °C) from open-channel current in the presence of 0·2 mM-internal Mg^{2+} and closed-state current. The square of the fluctuation amplitude (A^2 s) calculated using a fast Fourier transform is plotted against the frequency (Hz) using log–log coordinates. Insets under *a* and *b* show typical records of the open-channel current and closed-state current, respectively. The record illustrated in the middle shows the rising phase of open-channel current sampled at 50 kHz using point-plotting. During an interval of 10 μs (between two points, arrowheads), the current stepped from the base line to the open state, supporting the high fidelity of the recording system.

calculated from the closed current (*b* in Fig. 5) was much smaller compared to those of the open-channel current (usually less than 10^{-27} A^2 s), and gradually increased in the frequency region above 1 kHz. This increase in the background noise at higher frequencies was mainly attributable to the system noise including the recording apparatus and the preparations (for example, see Anderson & Stevens, 1973; Sigworth, 1985). The smooth increase of the background spectrum at higher frequencies suggests that the spectrum is not seriously deformed by limited frequency response of the recording system. This notion was supported by the rapid transition of the channel current examined at the higher time base (middle inset in Fig. 5).

In order to obtain the power-density spectrum of the current fluctuations induced

by blocking kinetics, the background noise spectrum was subtracted from that of open-channel currents. The difference spectra above 1 kHz gave a single Lorentzian component, which has been considered to be related to the steady-state conductance fluctuations following a first-order process (for review see Hille, 1984). Fig. 6 represents four power spectra thus obtained at 0 mV or +40 mV with 0·1 or 1·0 mM-internal Mg^{2+}, with the pipette containing 5·4 mM-K^+. The corner frequency (f_c, arrows in Fig. 6) at 1 mM-internal Mg^{2+} was increased as the membrane potential

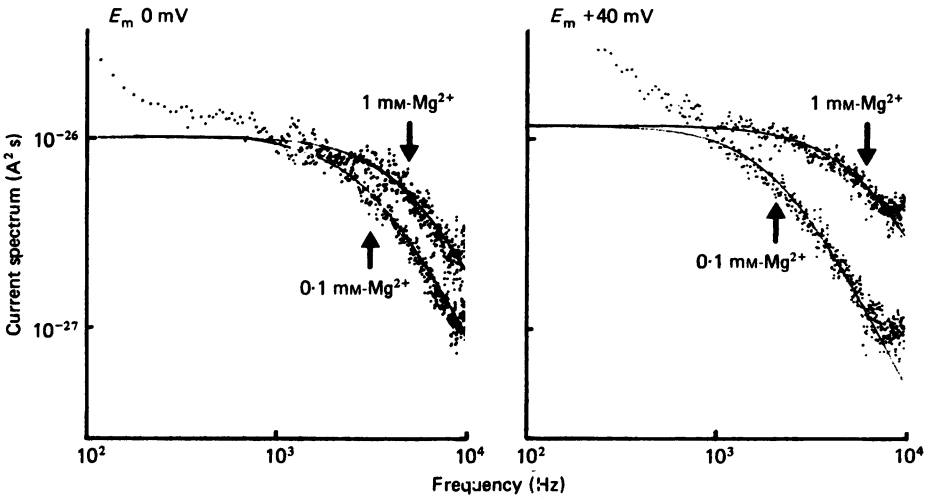

Fig. 6. Comparison of power-density spectra. Four difference spectra calculated from outward currents at $[K^+]_o$ 5·4 mM are shown in the same manner as in Fig. 5. The membrane potential of patches is indicated on each graph. Smooth lines are the least-squares fit of the equation: $S(f) = S(0)/(1+(f/f_c)^2)$ except at frequencies lower than 1 kHz. The arrows indicate the corner frequency (f_c) of each spectrum at which the power becomes half of $S(0)$. In the same graph, $S(0)$ was adjusted to the higher one for convenience of comparison. $S(0)$ ($\times 10^{-26}$ A^2s) and f_c (kHz) are respectively 0·5 and 3·1 with 0·1 mM-internal Mg^{2+}, 1·0 and 4·8 with 1 mM-internal Mg^{2+} at 0 mV; 0·9 and 2·7 with 0·1 mM-internal Mg^{2+}, 1·4 and 5·9 with 1 mM-internal Mg^{2+} at +40 mV. The power at lower frequencies was considered to be due to transitions between the open and closed states of the ATP-sensitive K^+ channel (Noma & Shibasaki, 1985), and was eliminated from the least-squares fitting of the curves.

was made more positive, whereas at 0·1 mM-internal Mg^{2+} it was reduced. Additional power spectra are seen in the frequency region less than 1 kHz. These powers were considered to be due to intrinsic transitions between the open and closed states of the ATP-sensitive K^+ channel (Noma & Shibasaki, 1985) and were excluded from analysis of blocking kinetics.

The values of f_c obtained at 5·4 mM-external K^+ were multiplied by 2π and plotted against the $[Mg^{2+}]_i$ values in Fig. 7*A*. The relationship between $2\pi f_c$ and $[Mg^{2+}]_i$ became steeper as the membrane potential was more positive, and the relations crossed at about 0·2 mM-internal Mg^{2+}. According to a model proposed in the next section, the slope of the lines gives the Mg^{2+} block rate (K_1) and the intersection with the ordinate gives its unblock rate (K_{-1}). Fig. 7*B* summarizes the corner frequency measured at +40 mV at three different levels of $[K^+]_o$. In parallel with raising $[K^+]_o$

from 0 to 20 mM, the corner frequency was increased at a given $[Mg^{2+}]_i$, although its scatter at 20 mM-external K^+ was considerable due to the limit of sampling domain (10 kHz).

A model for Mg^{2+} blockade of the ATP-sensitive K^+ channel

As two components have been observed in the closed-time histogram (Kakei *et al.* 1985), the channel should have at least two closed states. The transitions from the

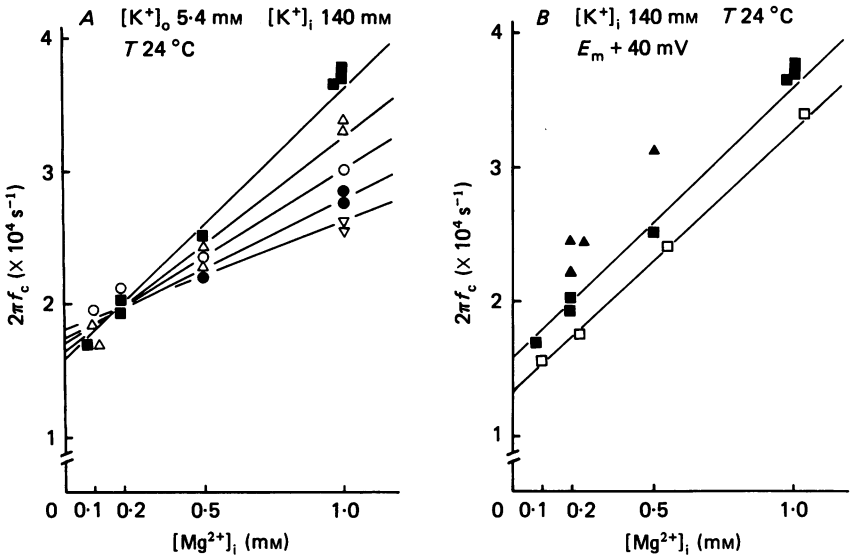

Fig. 7. Relationship between f_c and internal Mg^{2+}. *A*, the values of $2\pi f_c$ calculated from five patch-clamp experiments at $[K^+]_o$ 5·4 mM are plotted against $[Mg^{2+}]_i$. According to the linear eqn. (8), continuous lines were drawn by giving values of $a = 0{\cdot}28$ and $b = 0{\cdot}04$, so that the sum of a and b results in 0·32, since $\delta = a + b$ is known from the steady-state voltage ratio (see Fig. 8, $\ln((i_o/\bar{i}) - 1)$ *vs.* E_m) relations for Mg^{2+} blockade. ■, +40 mV; △, +20 mV; ○, 0 mV, ●, −20 mV; ▽, −40 mV. These theoretical lines corresponded well to the corner frequencies obtained experimentally. The slopes of these lines give the Mg^{2+} block rate (K_1) and the intersections with the ordinate its unblock rate (K_{-1}). At $[K^+]_o$ 5·4 mM, K_1 ($\times 10^7$ M^{-1} s^{-1}) and K_{-1} ($\times 10^4$ s^{-1}) are respectively 2·40 and 1·59 at +60 mV; 1·93 and 1·64 at +40 mV; 1·55 and 1·69 at 20 mV; 1·25 and 1·75 at 0 mV; 1·00 and 1·81 at −20 mV; 0·81 and 1·86 at −40 mV. *B*, the values of $2\pi f_c$ measured at +40 mV with three different levels of $[K^+]_o$ (0, 5·4 and 20 mM) are plotted against $[Mg^{2+}]_i$. The line fitted to the $[K^+]_o$ 0 mM data (□) was shifted to lower values in parallel with that measured at $[K^+]_o$ 5·4 mM (■) and gave the values of K_1 and K_{-1} at +40 mV of $1{\cdot}93 \times 10^7$ s^{-1} M^{-1} and $1{\cdot}33 \times 10^4$ s^{-1}, respectively. At $[K^+]_o$ 20 mM (▲) larger values of f_c were obtained at $[Mg^{2+}]_i$ 0·2 and 0·5 mM.

open state to the closed states are tentatively considered to be regulated by a binding of ATP to unknown binding site(s). To explain the blocking kinetics by Mg^{2+}, we simply assumed an additional blocked state following the open state,

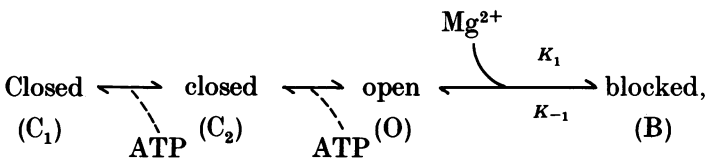

(2)

where K_1 is the second-order rate constant for Mg^{2+} binding ($M^{-1}\ s^{-1}$) and K_{-1} the first-order rate constant for unbinding (s^{-1}). Similar models have been used by other workers to explain an open-channel blocker (Armstrong, 1966, 1969; Heckmann, Lindemann & Schnakenberg, 1972; Woodhull, 1973). Based on the Eyring rate theory (Eyring, Lumry & Woodbury, 1949; Woodbury, 1971), the rate constants were given as:

$$K_1 = K_1' \exp(azE_m F/RT), \tag{3}$$

$$K_{-1} = K_{-1}' \exp(-bzE_m F/RT), \tag{4}$$

where K_1' and K_{-1}' are inversely proportional to the magnitude of the energy barrier against Mg^{2+} entry and exit through the inner mouth of the channel, and the other terms represent the influence of the transmembrane electrical field, E_m. According to constant-field theory (Goldman, 1943; Hodgkin & Katz, 1949), a is the partition parameter, which represents the fractional electrical distance between the inner mouth of the channel and the peak of the energy barrier, and b the distance between the energy barrier and the energy well of the Mg^{2+} binding site. Consequently, $\delta = a+b$ gives the electrical distance between the inner mouth and the Mg^{2+} binding site. z is the ionic valence. F, R and T have their usual meanings.

Assuming that the blocked state of the channel carries no current, $\bar{i}$ for the open-channel current is given by

$$\bar{i}/i_0 = O/(O+B), \tag{5}$$

where i_0 is the unit amplitude of the ATP-sensitive K^+ channel current measured in absence of internal Mg^{2+} and O and B are the probability of open and blocked states, respectively. Since the Hill coefficient was ~ 1, eqn. (5) can be formulated as

$$O/(O+B) = K_{-1}/(K_1[Mg^{2+}]_i + K_{-1}). \tag{6}$$

From eqns. (3), (4), (5) and (6),

$$\ln((i_0/\bar{i})-1) = \ln([Mg^{2+}]_i K_1'/K_{-1}') + (a+b)\,zE_m F/RT. \tag{7}$$

The corner frequency (f_c) of the Lorentzian spectrum is

$$2\pi f_c = K_1[Mg^{2+}]_i + K_{-1}. \tag{8}$$

According to this model, the data recorded by using 5·4 mM-K^+ pipette solution at 24 °C were analysed. To get a linear relationship between the mean amplitude and $[Mg^{2+}]_i$ as indicated by eqn. (7) $\ln((i_0/\bar{i})-1)$ was plotted against E_m at different levels of $[Mg^{2+}]_i$ in Fig. 8. The slope of the fitted lines gave δ ($= a+b$) of 0·32. In the experiment at 34 °C, δ was 0·30 (not shown in Figure). At $[K^+]_o$ of 0 and 20 mM (24 °C), δ was 0·31 and 0·32, respectively (not shown). The fraction of electrical drop for Mg^{2+} binding, therefore, appeared to be independent of both temperature and $[K^+]_o$.

The results of experiments could well be explained by the linear eqn. (8) as shown in Fig. 7. Two rate constants thus measured at $[K^+]_o$ 0 and 5·4 mM are summarized in Fig. 9. At different $[K^+]_o$ the Mg^{2+} block rate was little altered (●), but the unblock rate was increased by raising $[K^+]_o$ (○, △), suggesting that higher $[K^+]_o$ relieves the block of the channel by increasing the Mg^{2+} exit rate.

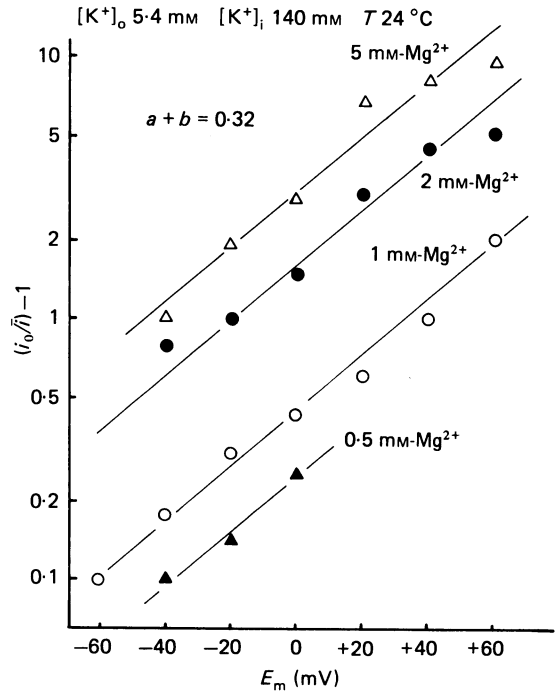

Fig. 8. Potential–ratio relationship of Mg^{2+} blockade. Parallel lines are fitted by eye to the semilog plots of $(i_0/\bar{i})-1$ *versus* membrane potential, thereby giving the electrical distance of Mg^{2+} binding site of $\delta = 0{\cdot}32$. At higher values of $[Mg^{2+}]_i$, the plots appear to bend slightly with increasing membrane potentials, reflecting the saturation of blocking effects. The line-fitting was therefore mainly performed between −40 mV and +40 mV at lower $[Mg^{2+}]_i$. Data were obtained from the same patch.

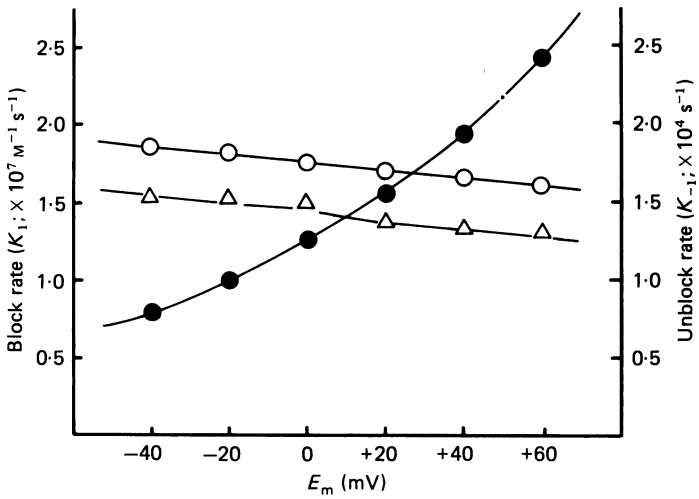

Fig. 9. Two rate constants governing Mg^{2+} blocking kinetics. Rate constants determined as described in Fig. 7 at $[K^+]_o$ 0 mM (triangles) and 5·4 mM (circles) are plotted against membrane potential. Compared to the unblock (or Mg^{2+} exit, open symbols) rate, the block (or Mg^{2+} entry, filled circles) rate is more steeply voltage dependent. Raising $[K^+]_o$ accelerated the Mg^{2+} exit while its entry rate remained almost unchanged.

Blockade of the ATP-sensitive K^+ channel by internal Na^+

Kakei *et al.* (1985) have suggested that the ATP-sensitive K^+ channel is blocked by Na^+ applied on the inner surface of the membrane. As it was found that the channel was unaffected by the external Na^+ (not shown), we examined whether the above model also accounts for the blocking effect of internal Na^+. The analysis was limited

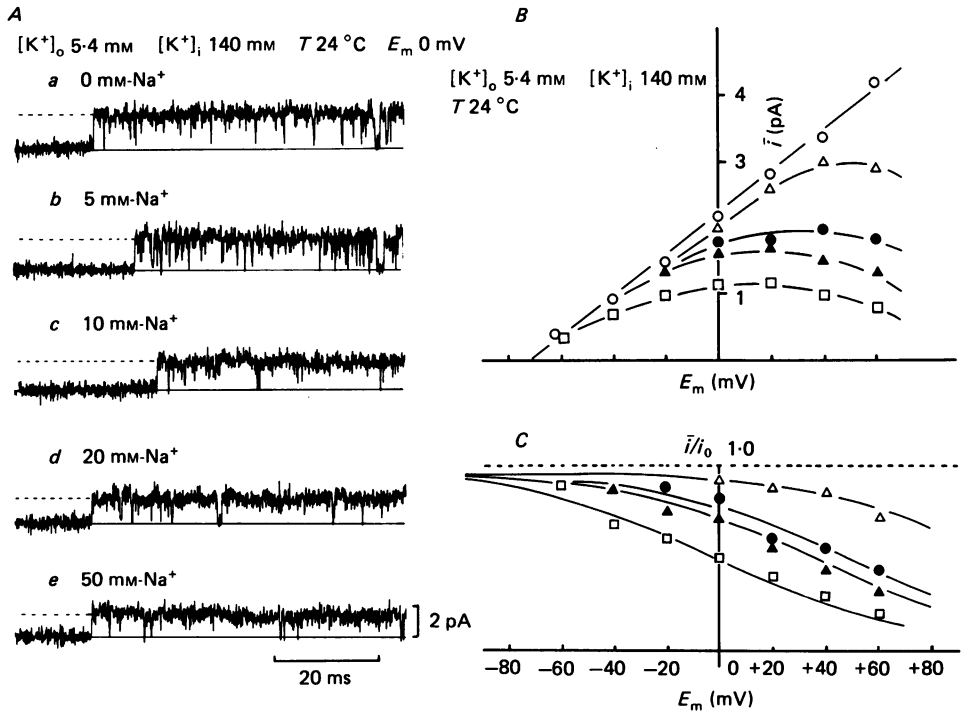

Fig. 10. Effect of internal Na^+ on outward currents. *A*, original current traces measured from the same patch at 0 mV with the internal solutions containing $[Na^+]_i$ of 0, 5, 10, 20 and 50 mM (24 °C). The pipette contained normal Tyrode solution ($[K^+]_o$ 5·4 mM). Continuous lines indicate the closed state, and dotted lines the open state of channel activity. Low-pass filter was 10 kHz. *B*, current–voltage relationships at various levels of $[Na^+]_i$ obtained from the current data shown in *A*. Symbols: ○, $[Na^+]_i$ 0 mM; △, 5 mM; ●, 10 mM; ▲, 20 mM; □, 50 mM. *C*, the ratios of mean currents ($\bar{i}/i_0$) are plotted against membrane potentials. Smooth lines are derived from saturation kinetics having a slope of $n = 2$ (cf. eqn. (1)), thereby giving a value for K_h of about 15 mM at +40 mV.

to the mean amplitude of the open-channel current, since the current flicker in the presence of internal Na^+ was too fast to be resolved with our recording system.

Original current traces and unitary current–voltage relations at various levels of $[Na^+]_i$ are illustrated in Fig. 10. When $[Na^+]_i$ was raised from 0 to 50 mM, the value of $\bar{i}$ for the outward current was reduced dose dependently as in the case of Mg^{2+} blockade, but its noise level was not significantly enhanced (Fig. 10*A* and *B*). Na^+ block became greater as the membrane potential was made more positive (Fig. 10*C*).

The dose–response relationships in Fig. 11*A* were fitted well by eqn. (1), having a Hill coefficient of $n = 2$, thereby resulting in a value of about 15 mM for K_h at

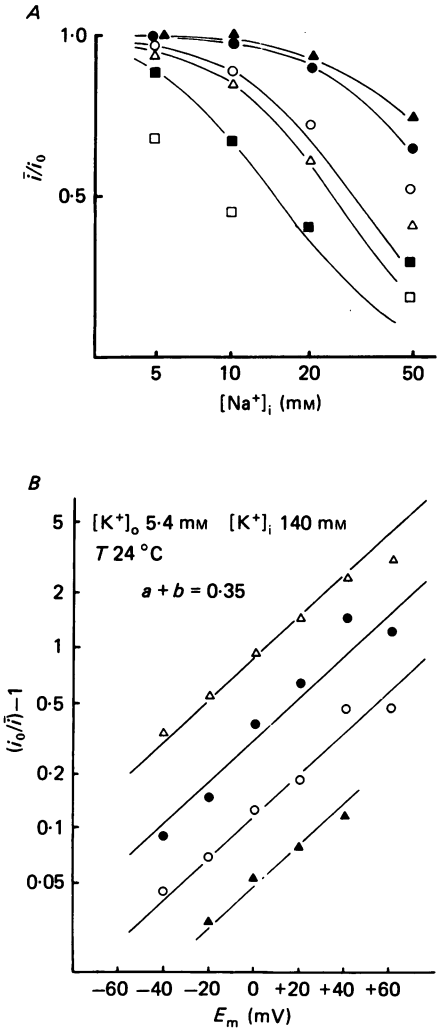

Fig. 11. Dose–response relationship and voltage dependence for Na^+ blockade. *A*, dose–response curves of Na^+ block are obtained by plotting the ratios of mean currents ($\bar{i}/i_0$) measured at various levels of $[Na^+]_i$ and fitting to eqn. (1); they show a sigmoidal decline in a dose- and voltage-dependent manner. Symbols: □, +60 mV; ■, +40 mV; △, +20 mV; ○, 0 mV; ●, −20 mV; ▲, −40 mV. *B*, ln $((i_0/\bar{i})-1)$ *versus* E_m relations for Na^+ blockade. The slope of parallel lines fitted by eye gives the value of electrical distance for the Na^+ binding site of $\delta = 0{\cdot}35$. Symbols: ▲, $[Na^+]_i$ 5 mM, ○, 10 mM; ●, 20 mM, △, 50 mM.

+40 mV. Na^+ concentration for half-maximum effect was at least 20-fold higher than that of Mg^{2+} block. In Fig. 11*B*, ln $((i_0/\bar{i})-1)$ *versus* E_m relationships were fitted well to the parallel lines with a slope determined with $\delta = 0{\cdot}35$, which is very similar to $\delta = 0{\cdot}32$ for the Mg^{2+} block. It was concluded that blocking sites of Na^+ and Mg^{2+} have similar electrical distances from the inner mouth of the channel, but a much higher concentration of Na^+ than Mg^{2+} is required to block the channel.

DISCUSSION

Flickery ionic block and inward rectification of the ATP-sensitive K^+ channel

It is well known that ionic flow through the K^+ channels is blocked by cations, such as Na^+, Li^+, Rb^+, TEA^+, Ba^{2+} and Sr^{2+} (Armstrong, 1966, 1969, 1971; Bergman, 1970; Bezanilla & Armstrong, 1972; French & Wells, 1977; Ohmori, 1978; Standen & Stanfield, 1978, 1980; Fukushima, 1982; Marty, 1983; Yellen, 1984*a*, *b*). In these studies the blocking particles are considered to enter the mouth of the channel pore, crossing an energy barrier, but they are unable to move on through the channel to the opposite side of the membrane because of another barrier(s). Thus, the blocking ions interfere with the passage of the permeable K^+ (multi-ion single-file channel pore, Hille & Schwartz, 1978).

The present study disclosed that internal Mg^{2+} as well as internal Na^+ at their physiological concentrations block the outward current through the ATP-sensitive K^+ channel. The results were well explained by an Eyring rate theory model with a binding site for Mg^{2+} at an electrical distance of about 0·32. The rapid flickery block of the elementary current results in an apparent inward rectification of the channel through a recording system with a limited frequency response.

In cultured bull-frog ganglion cells, the M-current relaxations normally seen with conventional micro-electrode voltage clamp was abolished using the whole-cell patch clamp with a pipette solution containing 5 mM-Mg^{2+}, but recovered when Mg^{2+} was omitted from the pipette solution, suggesting that intracellular Mg^{2+} blocked the M-current (Galvan, Satin & Adams, 1984). In single-channel recordings, Nowak, Bregestovski, Asher, Herbet & Prochiantz (1984) found that external application of Mg^{2+} blocked the inward-going current through the glutamate-activated channel in mouse cerebral neurones, voltage dependently. Although the direction of the block was opposite and the effective dose was slightly smaller (10–500 μM) than in the present study, the mechanism underlying the block (open-channel blocker) may be similar. Using planar lipid membrane technique, Nelson, Worley, Rogwers & Lederer (1985) observed a voltage-dependent and unidirectional Mg^{2+} block in single channels selective for both Na^+ and K^+, which were extracted from the calf ventricular muscle.

The dose–response relationships for Mg^{2+} and Na^+ block were well explained using conventional saturation kinetics (eqn. (1)). The location of the binding site for these blockers seems to be within the aqueous pore of the ATP-sensitive K^+ channel for two reasons, first, because the block was voltage dependent in such a way that it became greater when the membrane potential was shifted in the positive direction to drive blocking ions from the internal solution into the channel; secondly, the block of the channel was also dependent on the external K^+ concentration. When the net flux of K^+, i.e. the current through the channel, was inward the channel was not affected. The block was only seen when the flux was outward. This finding is explained by assuming a multi-ion, single-file pore channel having a binding site for Mg^{2+} within the channel as has been done in other studies (Fukushima, 1982; Yellen, 1984*a*).

How does external K^+ knock out Mg^{2+} from the binding site?

When we compare our original records at varying levels of $[K^+]_o$ (Fig. 4*A*), it is evident that the closed time is significantly longer at the lower concentration, and

the current level approaches the base line more closely (no channel open) during the flickery block, thereby causing the amplitude distribution with broader base. If external K^+, entering into the channel pore, competes with Mg^{2+} for the binding site, the block rate (K_1) will be decreased because of the reduced probability of Mg^{2+} binding. On the other hand, if external K^+ binds to one of multiple sites intrinsic to the channel of single-file property, which is located close to the Mg^{2+} binding site, and expels the blocking ion by electrostatic repulsive force, then the unblock rate (K_{-1}) will be increased.

According to the noise-analysis data derived from the single-channel currents (Figs. 7 and 9), the latter mechanism seems to be responsible for the relief of Mg^{2+} block of the ATP-sensitive K^+ channel, which is in line with the observations in the Ca^{2+}-activated K^+ channel by Yellen (1984*b*); using amplitude-distribution analysis, he found that raising external K^+ relieves Na^+ block of Ca^{2+}-activated K^+ channels in bovine adrenal medullary chromaffin cell membranes by increasing the Na^+ exit rate from the channel, not by competitively slowing its entry rate. By contrast, Standen & Stanfield (1978) attributed the relief by external K^+ of Ba^{2+} block of the inward rectifier K^+ channel in frog skeletal muscles to external K^+ competing for the saturable Ba^{2+} block site in the channel.

The external application of Mg^{2+} or Na^+ failed to block the ATP-sensitive K^+ channel. This finding clearly suggests that the channel has a barrier or barriers in the outer part of the channel and does not allow the blocking ions to enter the channel from the outer mouth.

Kakei & Noma (1984) measured elementary current–voltage relations at various levels of $[Na^+]_i$ replacing internal K^+ and found that the reversal potential was not changed, consistent with the idea of the selective site for K^+ over Na^+ and Mg^{2+}. In other channels, the relief of ionic block has been observed at extreme depolarizations (delayed rectifier K^+ channel: French & Wells, 1977) or hyperpolarizations (inward rectifier K^+ channel: Gay & Stanfield, 1977; Standen & Stanfield, 1980; Fukushima, 1982). These findings suggested that the strong electrical driving force expelled the blocking ion over its intrinsic energy barrier to the opposite side of membrane. In the present study we did not apply extreme depolarizations, but it appears that such a mechanism may also underlie the incomplete block of the channel observed when the membrane was extremely depolarized (Figs. 3 and 11). Kakei & Noma (1984) applied Ba^{2+} from the external side of the ATP-sensitive K^+ channel in the outside-out patch mode and found a block of the channel having quite slow kinetics, which suggests that Ba^{2+} can pass through the outer barrier(s) of the channel but at a low rate.

The kinetic basis of ionic block

The kinetics of the ionic block of the channel are dependent not only on the ionic species, but also on the kind of channel. The rate constant for Mg^{2+} blockade of the ATP-sensitive K^+ channel was around $1{\cdot}7 \times 10^7$ M^{-1} s^{-1} and the unblock rate was around $1{\cdot}8 \times 10^4$ s^{-1} ($[K^+]_o$ 5·4 mM). The values of these rate constants are rather similar to those of the block rate of $1{\cdot}4 \times 10^7$ M^{-1} s^{-1} and the unblock rate of $1{\cdot}1 \times 10^3$ s^{-1} for Mg^{2+} block of the cation channel (Nowak *et al.* 1984), and also similar to the block rate of about 7×10^6 M^{-1} s^{-1} and the unblock rate of about 7×10^4 s^{-1} for the Na^+ blockade of the Ca^{2+}-activated K^+ channel (Yellen, 1984*a*).

The rate constants for Na^+ blockade of the ATP-sensitive K^+ channel, on the other hand, appear to be larger than those of the above blocks. With our present technique it was impossible to determine the rate constants for Na^+ block. Fast or even 'instantaneous' block of channels by various alkaline metal ions has been reported in the delayed rectifier of the squid axon (Bezanilla & Armstrong, 1972; French & Wells, 1977) and in the inward rectifier K^+ channel of skeletal muscle fibres (Standen & Stanfield, 1980).

It is of interest that the block of the inward rectifier K^+ channel by Ba^{2+} is very slow, with a rate of the order of 10 s^{-1} (time constant for relaxation was 0·1–1·8 s; Standen & Stanfield, 1978). Similarly, Ba^{2+} block of the ATP-sensitive K^+ channel seems to be very slow (Kakei & Noma, 1984). The slow block of the inward rectifier is reported to occur not only with divalent cation Sr^{2+}, but also with monovalent cations such as Na^+ and Cs^+ in the tunicate egg cell (Fukushima, 1982). Thus, it is nearly impossible to relate these variable rate constants to crystal radii of the blocking ions. This variation in the rate constant indicates a presence of a selective filter of the type suggested by Bezanilla & Armstrong (1972) for the entry of these blocking ions into the channel.

The voltage dependence of the ionic block is mostly due to the block rate. The unblock rate is much less sensitive to the membrane potential but varies with external K^+ concentration in most systems, as in the case in our study.

In the present study the dose–response curves for Na^+ block were fitted with a slope of ~ 2, and those for Mg^{2+} block with a slope of ~ 1. Furthermore, the electrical distances were quite similar in both cases, ranging between 0·30 and 0·35. The most simple interpretation of this result is that Na^+ and Mg^{2+} share a common binding site for the channel blockade. However, in other systems, different sites are strongly suggested for Na^+ and Cs^+ (Fukushima, 1982), and Rb^+ and Cs^+ (Standen & Stanfield, 1980).

If the binding site has two negative charges and binds blocking cations, the positive charge will be neutralized. Then it is difficult to understand how the entry of external K^+ can knock out the blocking ions with electrostatic repulsive force. We cannot exclude the possibility that Na^+ and Mg^{2+} bind to an unknown blocking site, which is outside the ionic pathway of the channel and yet still sensitive to the electrical potential difference, and that these ions modulate the kinetics of the channel. Such an action of the blocking ions is assumed to be partially responsible for the Na^+ blocking of the Ca^{2+}-activated K^+ channel (Marty, 1983) and for the Mg^{2+} blockade of the cation channel (Nowak *et al.* 1984).

Physiological implications of the Mg^{2+} and Na^+ blockade

Intracellular free Mg^{2+} or Na^+ concentrations have been investigated using ion-sensitive electrodes and nuclear magnetic resonance (Hess, Metzger & Weingart, 1982; Gupta, Gupta & Moore, 1984; Blatter & McGuigan, 1986; Sheu & Fozzard, 1982). The reported concentrations were in the range 0·5–3·5 mM for Mg^{2+} and 5·0–9·0 mM for Na^+. These values indicate that the block of the ATP-sensitive K^+ channel observed in the present study is relevant to physiological conditions. Furthermore, in the ischaemic conditions where the open probability of ATP-sensitive K^+ channels is increased, internal free Mg^{2+} and Na^+ levels will be elevated as

a result of the release of Mg^{2+} bound to ATP and the accumulation of Na^+ due to the disturbed Na^+–K^+ pump activity.

It is still unknown whether the other cardiac K^+ channels, and the delayed rectifier and inward rectifier K^+ channels of the cardiac muscle are also affected by Na^+ and Mg^{2+}. However, the present study strongly suggests that cations, physiologically present in the cytoplasm, may play an important role in producing a low conductance of the outward K^+ current at plateau level of action potentials. Thus these cations may reduce the necessary size of the outward K^+ current, thereby minimizing metabolic expense for K^+ transport across the membrane.

The authors thank their colleagues at National Institute for Physiological Sciences and Dr N. B. Standen, Department of Physiology, University of Leicester, for stimulating discussions and valuable comments during the preparation of the manuscript. One of the authors (M. H.) also thanks Professor C. Kawai, the Third Department of Internal Medicine, Kyoto University, for providing him with an opportunity to work at the National Institute for Physiological Sciences. The work was carried out with the excellent technical help of Mr M. Ohara and Mr O. Nagata. This work was supported by a research grant from the Ministry of Education, Science and Culture of Japan. M. H. is a Postgraduate Fellow of the Japan Society for Promotion of Sciences.

REFERENCES

ANDERSON, C. R. & STEVENS, C. F. (1973). Voltage clamp analysis of acetylcholine produced end-plate current fluctuations at frog neuromuscular junction. *Journal of Physiology* **235**, 655–691.

ARMSTRONG, C. M. (1966). Time course of TEA^+-induced anomalous rectification in squid giant axon. *Journal of General Physiology* **50**, 491–503.

ARMSTRONG, C. M. (1969). Inactivation of the potassium conductance and related phenomena caused by quaternary ammonium ion injected in squid axon. *Journal of General Physiology* **54**, 552–575.

ARMSTRONG, C. M. (1971). Interaction of tetraethylammonium ion derivatives with the potassium channels of giant axons. *Journal of General Physiology* **58**, 413–437.

ASHCROFT, F. M., HARRISON, D. E. & ASHCROFT, S. H. (1984). Glucose induces closure of single potassium channels in isolated rat pancreatic β cells. *Nature* **312**, 446–448.

BERGMAN, C. (1970). Increase of sodium concentration near the inner surface of nodal membrane. *Pflügers Archiv* **317**, 287–302.

BEZANILLA, F. & ARMSTRONG, C. M. (1972). Negative conductance caused by entry of sodium and cesium ions into the potassium channels of squid axons. *Journal of General Physiology* **60**, 588–608.

BLATTER, L. A. & MCGUIGAN, J. A. S. (1986). Free intracellular magnesium concentration in ferret ventricular muscle measured with ion selective micro-electrodes. *Quarterly Journal of Experimental Physiology* **71**, 467–473.

COLQUHOUN, D. (1971). *Lectures on Biostatistics*. Oxford: Clarendon Press.

COOK, D. L. & HALES, C. N. (1984). Intracellular ATP directly blocks K^+ channels in pancreatic *B*-cells. *Nature* **311**, 271–273.

EYRING, H., LUMRY, R. & WOODBURY, J. W. (1949). Some applications of modern rate theory to physiological systems. *Record of Chemical Progress* **10**, 100–114.

FABIATO, A. & FABIATO, F. (1979). Calculator programs for computing the composition of the solutions containing multiple metals and ligands used for experiments in skinned muscle cells. *Journal de Physiologie* **75**, 463–505.

FRENCH, R. J. & WELLS, J. B. (1977). Sodium ions as blocking agents and charge carriers in the potassium channel in the squid axon. *Journal of General Physiology* **70**, 707–724.

FUKUSHIMA, Y. (1982). Blocking kinetics of the anomalous potassium rectifier of tunicate egg studied by single channel recording. *Journal of Physiology* **331**, 311–331.

GALVAN, M., SATIN, L. S. & ADAMS, P. R. (1984). Comparison of conventional microelectrode and whole-cell patch clamp recordings from cultured bullfrog ganglion cells. *Society for Neuroscience Abstracts* **10**, 44.

GAY, L. A. & STANFIELD, P. R. (1977). Cs causes a voltage-dependent block of inward K currents in resting skeletal muscle fibres. *Nature* **267**, 169–170.

GOLDMAN, D. E. (1943). Potential, impedance, and rectification in membranes. *Journal of General Physiology* **27**, 37–60.

GUPTA, R. K., GUPTA, P. & MOORE, R. D. (1984). NMR studies of intracellular metal ions in intact cells and tissues. *Annual Review of Biophysics and Bioengineering* **13**, 221–246.

HAGIWARA, S. & YOSHII, M. (1980). Effects of temperature on the anomalous rectification on the membrane of the egg of the starfish *Mediaster aqeualis*. *Journal of Physiology* **307**, 517–527.

HAMILL, O. P., MARTY, A., NEHER, E., SAKMANN, B. & SIGWORTH, F. J. (1981). Improved patch-clamp techniques for high-resolution current recordings from the cells and cell-free membrane patches. *Pflügers Archiv* **391**, 85–100.

HECKMANN, K., LINDEMANN, K. & SCHNAKENBERG, J. (1972). Current–voltage curves of porous membranes in the presence of pore-blocking ions. I. Narrow pores containing no more than one moving ion. *Biophysical Journal* **12**, 683–702.

HESS, P., METZGER, P. & WEINGART, R. (1982). Free magnesium in sheep, ferret and frog striated muscle at rest measured with ion-selective micro-electrode. *Journal of Physiology* **333**, 173–188.

HILLE, B. (1984). *Ionic Channels of Excitable Membranes*. Sunderland, MA, U.S.A.: Sinauer Associates Inc.

HILLE, B. & SCHWARZ, W. (1978). K channels as multi-ion single-file pores. *Journal of General Physiology* **72**, 409–442.

HODGKIN, A. L. & KATZ, B. (1949). The effect of sodium ions on the electrical activity of the giant axon of the squid. *Journal of Physiology* **108**, 37–77.

HORIE, M., NOMA, A. & IRISAWA, H. (1986). Intracellular Mg^{2+} and Na^+ block outward current through ATP-regulated K^+ channel in guinea-pig ventricular cells. *Proceedings of the International Union of Physiological Sciences* **16**, 231.

ISENBERG, G. & KLÖCKNER, U. (1982). Calcium tolerant ventricular myocytes prepared by preincubation in a 'KB medium'. *Pflügers Archiv* **395**, 6–18.

KAKEI, M. & NOMA, A. (1984). Adenosine-5′-triphosphate-sensitive single potassium channel in the atrioventricular node cell of the rabbit heart. *Journal of Physiology* **352**, 265–284.

KAKEI, M., NOMA, A. & SHIBASAKI, T. (1985). Properties of adenosine-triphosphate-regulated potassium channels in guinea-pig ventricular cells. *Journal of Physiology* **363**, 441–462.

MARTY, A. (1983). Blocking of large unitary calcium-dependent potassium currents by internal sodium ions. *Pflügers Archiv* **396**, 179–181.

NELSON, M. T., WORLEY, J. F., ROGWERS, T. B. & LEDERER, W. J. (1985). Magnesium blockade of a cation-sensitive, rectifying channel from heart muscle. *Biophysical Journal* **47**, 143a.

NOMA, A. (1983). ATP-regulated K channels in cardiac muscle. *Nature* **305**, 147–148.

NOMA, A. & SHIBASAKI, T. (1985). Membrane current through adenosine-triphosphate-regulated potassium channels in guinea-pig ventricular cells. *Journal of Physiology* **363**, 463–480.

NOWAK, L., BREGESTOVSKI, P., ASCHER, P., HERBET, A. & PROCHIANTZ, A. (1984). Magnesium gates glutamate-activated channels in mouse central neurones. *Nature* **307**, 462–465.

OHMORI, H. (1978). Inactivation kinetics and steady-state current noise in the anomalous rectifier of tunicate egg cell membranes. *Journal of Physiology* **281**, 77–99.

POWELL, T., TERRAR, D. A. & TWIST, V. W. (1980). Electrical properties of individual cells isolated from adult rat ventricular myocardium. *Journal of Physiology* **302**, 131–153.

RORSMAN, P. & TRUBE, G. (1985). Glucose dependent K^+ channels in pancreatic β-cells are regulated by intracellular ATP. *Pflügers Archiv* **405**, 305–309.

SHEU, S. S. & FOZZARD, H. A. (1982). Transmembrane Na^+ and Ca^{2+} electrochemical gradients in cardiac muscle and their relationship to force development. *Journal of General Physiology* **80**, 325–351.

SIGWORTH, F. J. (1985). Open channel noise. I. Noise in acetylcholine receptor currents suggests conformational fluctuations. *Biophysical Journal* **47**, 709–720.

SPRUCE, A. E., STANDEN, N. B. & STANFIELD, P. R. (1985). Voltage-dependent ATP-sensitive potassium channels of skeletal muscle membrane. *Nature* **316**, 736–738.

STANDEN, N. B. & STANFIELD, P. R. (1978). A potential- and time-dependent blockade of inward rectification in frog skeletal muscle fibres by barium and strontium ions. *Journal of Physiology* **280**, 169–191.

STANDEN, N. B. & STANFIELD, P. R. (1980). Rubidium block and rubidium permeability of the inward rectifier of frog skeletal muscle fibres. *Journal of Physiology* **304**, 415–435.

TANIGUCHI, J., KOKUBUN, S., NOMA, A. & IRISAWA, H. (1981). Spontaneously active cells isolated from the sino-atrial and atrio-ventricular nodes of the rabbit heart. *Japanese Journal of Physiology* **31**, 547–558.

TRUBE, G. & HESCHELER, J. (1984). Inward-rectifying channels in isolated patches of the heart cell membranes: ATP-dependence and comparison with cell-attached patches. *Pflügers Archiv* **401**, 178–184.

TSIEN, R. Y. & RINK, T. J. (1980). Neutral carrier ion-selective microelectrodes for measurement of intracellular free calcium. *Biochemica et biophysica acta* **599**, 623–638.

WOODBURY, J. W. (1971). Eyring rate theory model of the current–voltage relationships of ion channels in excitable membranes. In *Chemical Dynamics*, ed. HIRSCHFELDEN, J. O., pp. 601–617. New York: John Wiley.

WOODHULL, A. M. (1973). Ionic blockade of sodium channel in nerve. *Journal of General Physiology* **61**, 687–708.

YELLEN, G. (1984*a*). Ionic permeation and blockade in Ca^{2+}-activated K^+ channels of bovine chromaffin cells. *Journal of General Physiology* **84**, 157–186.

YELLEN, G. (1984*b*). Relief of Na^+ block of Ca^{2+}-activated K^+ channels by external cations. *Journal of General Physiology* **84**, 187–199.